eJSE International

EJSE Special Issue: Sensor Network on Building Monitoring: from theory to real application (2009)

Active Ultra-Wideband Tag Design for Concrete Debris Tracking Systems

Y. Z. Shen±
C. L. Law*
K. S. Koh
S. M. Hu
School of Electrical and Electronic Engineering, Nanyang Technological University, Singapore

*Email: sh0001hu@ntu.edu.sg±; ecllaw@ntu.edu.sg**

ABSTRACT: Compared with the traditional high-speed video camera measurement method, ultra-wideband (UWB) technology is valuable in the detection and tracing of debris throw during explosion, due to its distinct advantages such as high positioning accuracy, multipath immunity, and low power consumption. In this paper, dielectric properties of Concrete slabs are first measured and used in the design of a slot antenna embedded in Concrete. An active UWB tag integrated with the slot antenna is designed for a real-time debris tracking system. The tag size is 25 × 25 × 25 mm which can be embedded in Concrete. Due to its small size, the tag has high chance to be intact in fragmented Concrete debris in explosion. The tag has low DC power consumption of 22.8 mW with output pulse amplitude of 12 V peak to peak (into 50 ohms) resulting in operating range of more than 190 meters.

KEYWORDS: Active tags, antennas, concrete, debris tracking system, ultra-wideband (UWB).

1 INTRODUCTION

In the experiment of debris throw tracking of Concrete under high explosives, traditionally high-speed digital video cameras are employed to record the process. Several cameras are used during the tests for different functions. Some are dedicated to register the break-up process of the Concrete wall, while others record the launch velocity and angles, or any possible bounce and roll of Concrete debris. All images are used to compose a break-up pattern. Finally, post processing is made to determine debris mass size distribution and location (Foger et al. 2006).

However, the usage of cameras has many limits as it cannot capture debris tracking in nighttime without light, or behind some obstacles. Furthermore, due to the very large amount of data registered in cameras, it becomes difficult to evaluate comparisons like launch angles versus debris size and loading density, as well as debris velocity versus debris size and travelling distance.

Recently, ultra-wideband (UWB) technology has been widely studied for real-time localization with high positioning accuracy (Gezici et al. 2005). UWB is a radio frequency technology having transmitted signal bandwidth exceeding 500 MHz or 20% of the center carrier frequency. The Federal Communications Commission (FCC) authorized the UWB signal transmissions in the range from 3.1 to 10.6 GHz (FCC 2002) in multiple bands with the lower-band from 3.1 to 4.85 GHz.

In our project, lower-band UWB technology is employed. Hundreds of compact UWB tags (transmitters) are embedded in Concrete before explosion. Instead of using high speed camera to capture images, UWB sensors (receivers) at hundreds of meters away are employed to receive signals transmitted by the tags. Subsequently, the received raw data are processed by positioning algorithm for real-time debris identification and trajectory tracking. The proposed method is immune to multipath effect, independent of weather and light, and can easily identify and track specific Concrete debris containing the UWB tags. Therefore, this method has many advantages compared with traditional cameras.

Nevertheless, there are many challenging problems to be solved for this kind of system, especially on the design of the active UWB tag. Firstly, as mentioned above, the tags including antennas are buried in Concrete in our project. It is well-known that the antenna characteristics such as input impedance and radiation pattern are sensitive to its environment, especially the near-field region. Therefore, the dielectric characteristics of Concrete and its effect on the antenna performance should be carefully investigated. Secondly, the active tags including antenna, circuits, and battery should be compact enough to be casted into a Concrete wall of less than 10 cm thick during fabrication. In particular, the

whole active tag size is required to be within 25 × 25 × 25 mm to have a fairly high chance that the fragmented Concrete wall in explosion will have debris bigger than the tag size and hence the complete tag can be intact in the debris. Thirdly, in order to enhance the detection range of the debris tracking system, the UWB pulses transmitted by the active UWB tags should be with high peak-to-peak amplitude of greater than 12 Volts. Fourthly, due to the limited battery size, low power consumption of the active tag is also necessary.

In this paper, the dielectric characteristics of three Concrete samples are measured in the frequency domain in Section 2. Based on this study, a UWB antenna embedded in Concrete is then proposed and optimized with the measured dielectric constant (ε_r) and loss tangent ($\tan\delta$). Section 3 shows the geometry of the proposed antenna, and dielectric property effects of Concrete on antenna performance. In Section 4, the performance of the fabricated antenna is investigated both in time and frequency domains. Section 5 introduces the circuit blocks in the entire active UWB tag. Finally, conclusions are presented in Section 6.

2 DIELECTRIC PROPERTIES OF CONCRETE

2.1 *Measurement setup*

The material parameters such as dielectric constant and loss tangent determine the signal propagation characteristics through the material. In addition, the antenna characteristics changes with the material around it. Thus, the dielectric constant and loss tangent of Concrete for all frequencies across the UWB signal band are required for the design of UWB antenna embedded in Concrete and for prediction of signal attenuation propagating through Concrete. Unfortunately, these parameters for Concrete are not readily available in the literature and hence measurements are conducted to obtain them. Traditionally, there are two kinds of measurement techniques: frequency and time domain measurement (Aurand 1996). The time-domain technique is more straightforward for transient measurements; nevertheless, it is difficult to obtain frequency-domain characteristics. On the contrary, the frequency-domain technique is with higher accuracy; moreover, since UWB occupies large frequency range, the frequency-dependent characteristics of Concrete should be investigated. Therefore, in this paper, the frequency-domain method is employed, and illustrated as follows.

As shown in Fig. 1, a moving metallic screen covered with electromagnetic wave absorbing materials is employed, with a transmission window of 40 × 40 cm in the center which is covered with a Concrete slab. Two transversal electromagnetic (TEM) horn antennas are fixed at equal distance from the centre of the screen at 2.1 m apart to meet the far-field requirement of the antenna. A vector network analyzer (VNA) is used to control the frequency sweep from 2 to 6 GHz and obtain the frequency response. Three Concrete slabs with different thickness of 4 cm, 7 cm, and 10 cm are used for comparison.

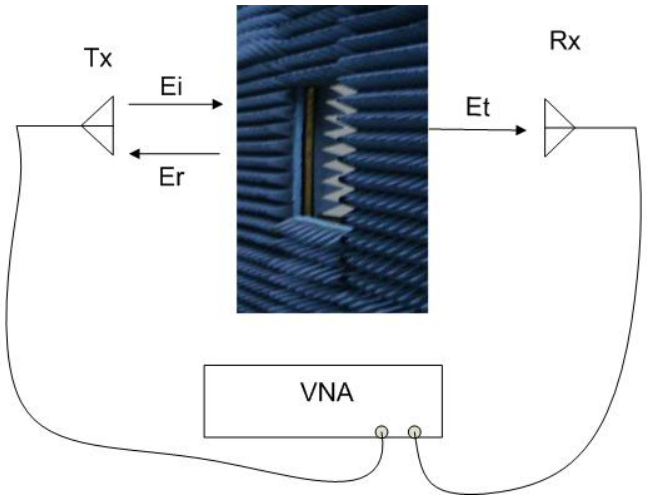

Figure 1. Measurement setup.

2.2 *Measurement results*

The frequency-domain measurement technology is based on the transfer function defined as the ratio of two S-parameters: $S_{21}(f)$ in the presence of the Concrete slab to cover the window in metallic screen and $S_{21}^{fs}(f)$ in free space without the Concrete slab.

First, the inverse fast Fourier transform (IFFT) is employed to the two measured $S_{21}(f)$ and $S_{21}^{fs}(f)$. Hamming window is chosen to remove the noise beyond the antenna bandwidth, and time-gating is used to remove the ringing in the time-domain waveforms due to reflections. After that, fast Fourier transform (FFT) is employed to transform the time gated results back into frequency-domain. The complex dielectric constant (ε_r) and loss tangent ($\tan\delta$) can be computed from the transfer function using single-pass analysis method (Muqaibel et al. 2005). Details about the measurement process and time-domain results can be found in (Shen et al. 2008).

The measured frequency-dependent dielectric constant and loss tangent results are shown in Fig. 2 and Fig. 3, respectively. The variation of dielectric constant and loss tangent among the three Concrete slabs with different thickness is due to two possible reasons: firstly, the three Concrete slabs could not be absolutely identical with each other because of non-uniform proportion of mix of many materials such as

stone and sand in the Concrete slab; secondly, the dielectric property is sensitive to the water content in those Concrete samples.

Finally, based on the results shown in Fig. 2 and Fig. 3, the average values of dielectric constant of 8.16 and loss tangent of 0.33 are chosen for the embedded antenna design in the following section.

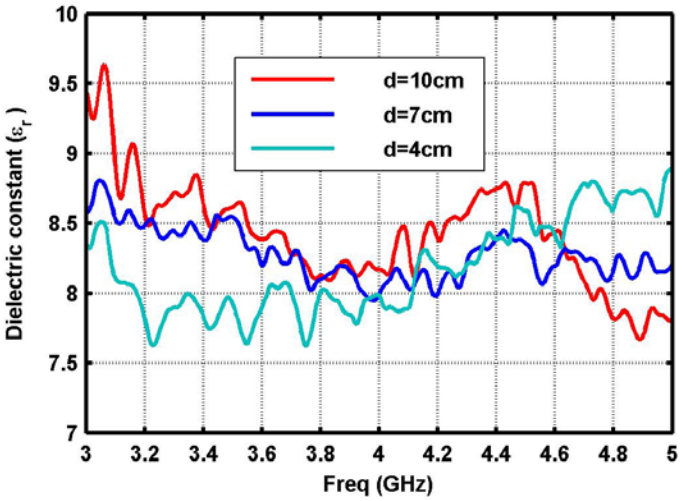

Figure 2. Measured dielectric constant of three Concrete slabs with different thickness *d*.

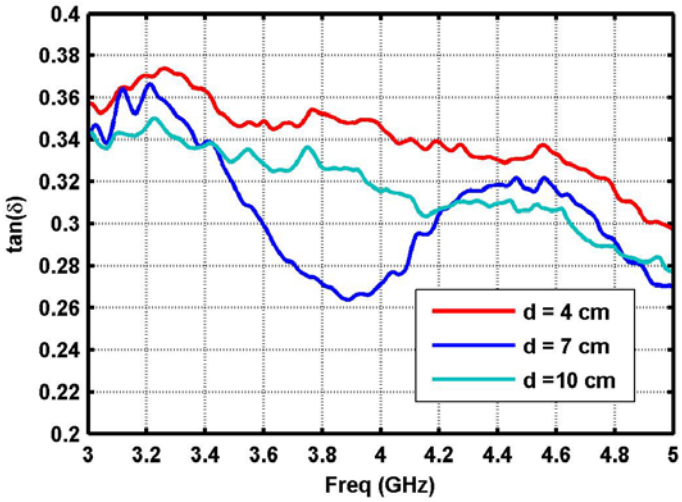

Figure 3. Measured loss tangent of three Concrete slabs with different thickness *d*.

3 UWB ANTENNA EMBEDDED IN CONCRETE

3.1 *Antenna geometry*

The proposed antenna with compact size of 25 × 25 mm is printed on a square substrate material of RO4003C, with relative dielectric constant of 3.38 and thickness of 0.508 mm. It is composed of a truncated corner and a grounded inverted-L strip at the two opposite corners, and a two-step impedance transformer, based on a previous study of slot antenna (Szw et al. 2008).

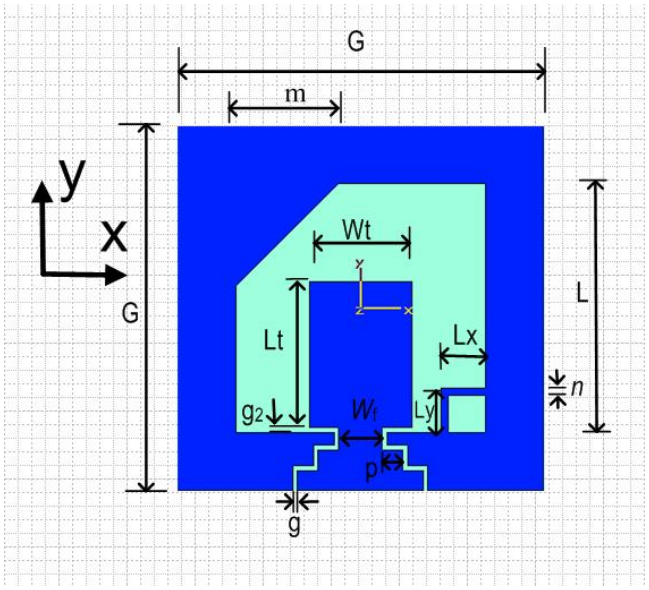

Figure 4. Geometry of the UWB slot antenna embedded in Concrete.

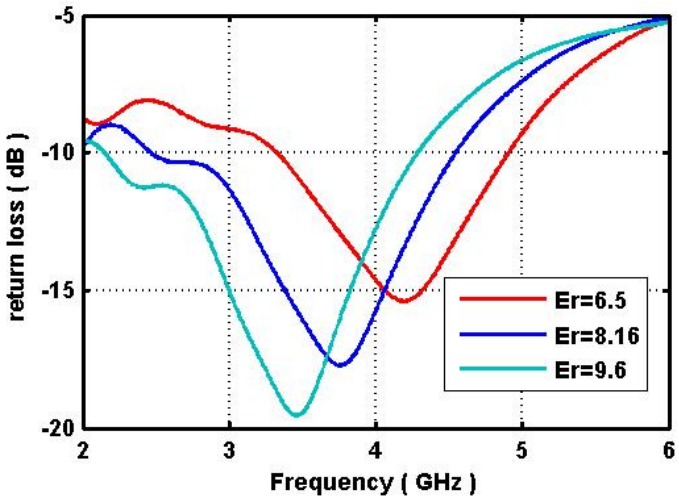

Figure 5. Simulated return loss of the UWB slot antenna embedded in Concrete with different complex dielectric constant.

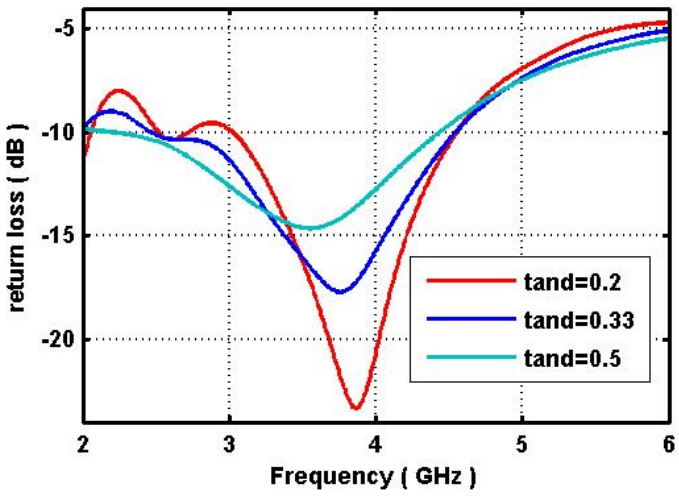

Figure 6. Simulated return loss of the UWB slot antenna embedded in Concrete with different loss tangent.

As shown in Fig. 4, the antenna is fed by a coplanar waveguide (CPW) line with a signal strip of width W_f, two equal square steps of p as impedance transformer, and two identical gaps of g between itself and coplanar ground plane. The strip line is protruded into the square slot of side length L with length of $Lt+g2$ and width of Wt. The length of the truncated corner is m, and the inverted-L strip has a length of Lx and Ly with width of n.

3.2 *Effect of Concrete*

The effect of Concrete on the antenna performances is studied through simulations assuming another dielectric layer covering the antenna with dielectric constant of 8.16 and loss tangent of 0.33. These are averaged values obtained from the measurement results of Concrete samples discussed in Section 2. However, as discussed in Section 2.2, the dielectric constant and loss tangent values may vary and it is important to ensure that the performance of the antenna is acceptable over the range of variation. Therefore, the sensitivity of the antenna performance on dielectric constant and loss tangent variations is also studied by simulation.

As shown in Fig. 5, the resonant frequency shifts to lower frequency with the increase of dielectric constant. The resonant frequency changes by 20% when the dielectric constant changes by 38%. Meanwhile, as shown in Fig. 6, the return loss of the proposed antenna is not sensitive to loss tangent variations, except at the resonant frequency. The results also show that the effect of Concrete is twofold: on one hand, due to its high $\tan\delta$, the Concrete will obviously attenuate the antenna radiated signal strength; on the other hand, compared with the free-space antenna design, the antenna embedded in Concrete can be smaller because of the large ε_r, which makes the Concrete work as a Superstrate in the antenna design.

4 ANTENNA CHARACTERISTICS

4.1 *Return loss*

After optimization, the dimensions of the final antenna design are: G = 25 mm, L = 17 mm, W_t = 7 mm, L_t = 10 mm, L_x = L_y = 3 mm, n = 0.5 mm, W_f = 3 mm, g = g_2 = 0.3 mm, m = 7 mm, p = 1.4 mm. This antenna is fabricated and embedded in Concrete with thickness of 4 cm as shown in Fig. 7.

As shown in Fig. 8, the measured 10-dB return loss frequency band is similar to simulated one which is from 2.7 to 4.5 GHz, or about 50% referenced to the center frequency of 3.6 GHz. The discrepancies between simulated and measured results are due to the fabrication tolerance of the fabricated antenna prototypes, the additional coaxial feed line shown in Fig. 7, and the aforementioned factors mentioned in Section 3.2 that the surrounding Concrete are not exactly with $\tan\delta$ of 0.33 and ε_r of 8.16.

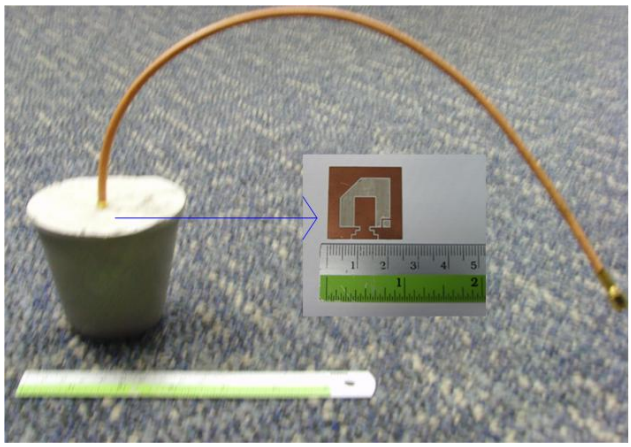

Figure 7. Fabricated UWB slot antenna embedded in Concrete.

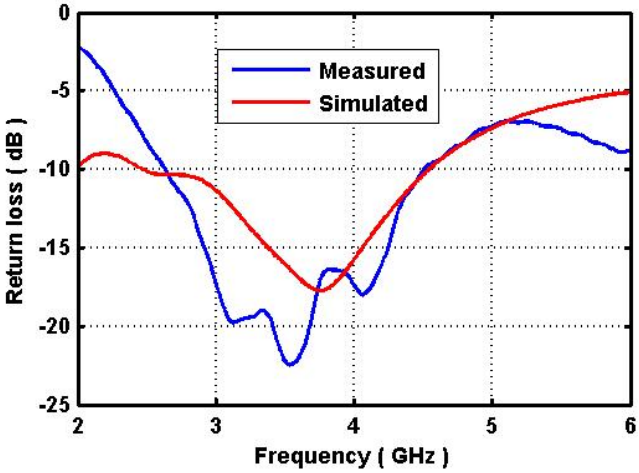

Figure 8. Measured and simulated return loss of the slot UWB antenna embedded in Concrete.

4.2 *Time-domain performance*

In localization application, the time domain pulse response of the antenna is important, so the proposed antenna is also measured in time domain with UWB pulse excitation. The measurement setup is shown in Fig. 9. A linearly polarized tapered slot antenna (Hu et al. 2009) fed by a pulse generator with operating range of 3.5 to 5 GHz and a power amplifier is used as the transmitter, while the proposed antenna embedded in Concrete is used as a receiver. The distance between the two antennas is chosen as 1.7 m to be in the far-field. The transmitter antenna is rotated in the *x-y* plane (varying Φ) to determine the circular polarization properties of the receiving antenna. Subsequently, the receiving antenna is rotated in the *x-z* plane (varying θ) to determine the azimuth plane radiation pattern of the receiving antenna.

In the *x-y* plane of the proposed antenna, the measured results in Fig. 10 (a) show that the amplitude and waveform vary with Φ from 0^o to 180^o. The maximum normalized peak-to-peak amplitude is 1.931 at $\Phi = 90^o$, while the minimum one is 0.986 at $\Phi = 0^o$, which corresponds to 51.1% (-5.83 dB) decrease.

Fig. 10 (b) shows the measured radiation variation in *x-z* plane of the embedded antenna. The largest normalized peak-to-peak amplitude of 1.951 occurs at $\theta = 0^o$, decreasing to 1.502 (-2.27 dB) at $\theta = 40^o$, and finally reaches the minimum one of 0.923 (-6.51 dB) at $\theta = 90^o$. These time domain measurement results demonstrate that the proposed antenna can receive signals both in *x-y* and *x-z* plane, which will improve the signal reception for different orientation and direction of the debris with respect to the tracking system receivers.

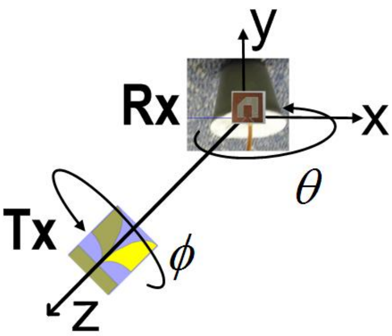

Figure 9. Time domain measurement setup.

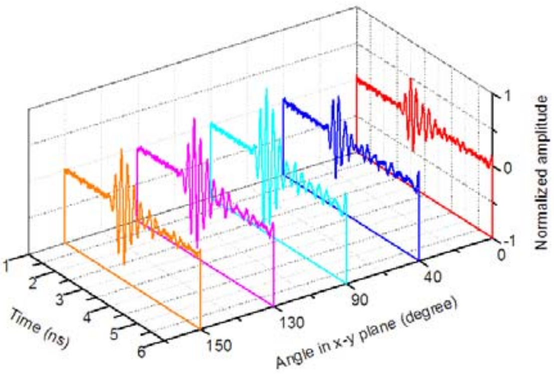

(a)

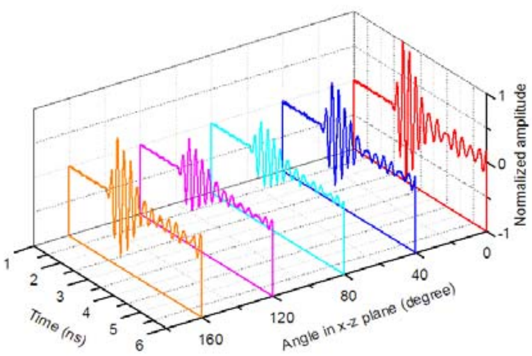

(b)

Figure 10. Measured waveforms received by the antenna embedded in Concrete: (a) varying Φ whereas $\theta = 0^o$, (b) varying θ whereas $\Phi = 90^o$.

5 ACTIVE UWB TAG DESIGN

5.1 *The active tag design*

Following the design of UWB antenna embedded in Concrete as shown in above, an active tag is developed and its schematic is shown in Fig. 11. The main fabricated functional blocks are illustrated in Fig. 12 (a). These functional blocks are then covered with Silicone rubber for water proofing, and integrated to form an active UWB tag as shown in Fig. 12 (b). Finally, as shown in Fig. 12 (c), the entire tag is embedded in Concrete block of 7 × 7 × 7 cm for testing. The external wires are used as switches to power on/off the embedded active tag.

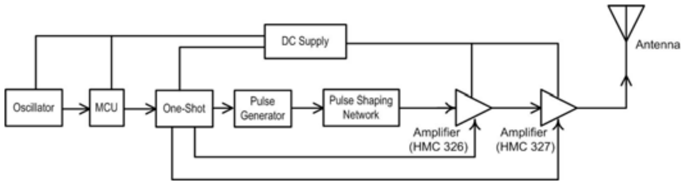

Figure 11. The schematic of a active UWB tag.

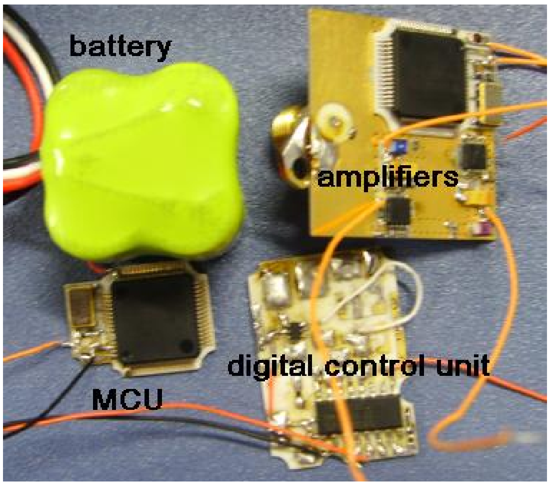

(a)

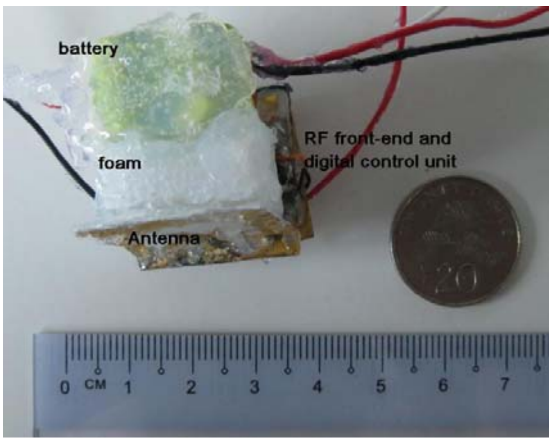

(b)

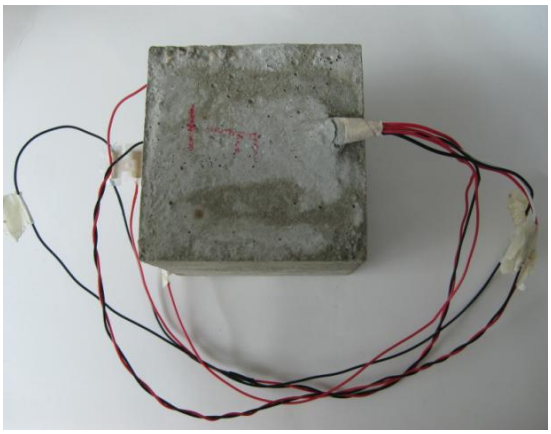

(c)

Fig. 12. The fabricated active UWB tag: (a) part of separated functional blocks, (b) integrated design covered by Silicone rubber, and (c) an active tag embedded in Concrete.

One of the most distinct advantages of the active UWB tag is its compact size of only 25 × 25 × 25 mm, as shown in Fig. 12 (b). This is achieved by employing multilayer technique. Moreover, Strip line rather than Microstrip line or Coplanar waveguide is adopted to dramatically reduce the layout size of the radio frequency (RF) front-end, especially the pulse shaping network and two amplifiers parts.

Another key advantage of the tag is its low power consumption with high output power. In order to power up the active tag from small size battery, the pulse repetition frequency (PRF) of the active tag is chosen to be as low as 200 kHz, because the reduction in PRF will result in lower power consumption. Furthermore, both the pulse width and pulse delay must be carefully controlled to maximize the final output amplitude of the active tag and minimize the power consumption. Thus a digital control circuit shown in Fig. 13 is designed and illustrated as follows.

Firstly, the PRF of an active tag is determined by the oscillator and the codes preloaded into the microcontroller unit (MCU). As shown in Fig. 13, the clock signal from the MCU will then be used to trigger the multi-vibrator (one-shot) at node 2. Secondly, by adjusting the external resistors R1, R2 and capacitor values C3, the output pulse width at nodes 12 and 13 can be tuned correspondingly. This tuning is very important, because the current consumption increases with the width of the generated pulse. Thirdly, the pulse delay needs to be adjusted correctly such that the amplifier is turned on for a momentary period just when the pulses arrive at it.

Both the required pulse width and pulse delay can be obtained experimentally by using a programmable pulse generator (Taber Electronics 8600) to manually tune the pulse width and the delay of the pulse into the two amplifiers at nodes 12 and 13 for the desired result of highest output amplitude at the lowest current consumption. The implemented pulse width and delay control circuit is shown in Fig. 13. The required pulse width of 30 nS to be connected to the power down of the amplifier (Hittite HMC326) at node 12 is set through the 2k ohms resistor R2. The following amplifier (Hittite HMC327) at node 13 is also powered up by a 30 nS pulse which is controlled by the 3k ohms resistor R1 and the 12 pF capacitor C3.

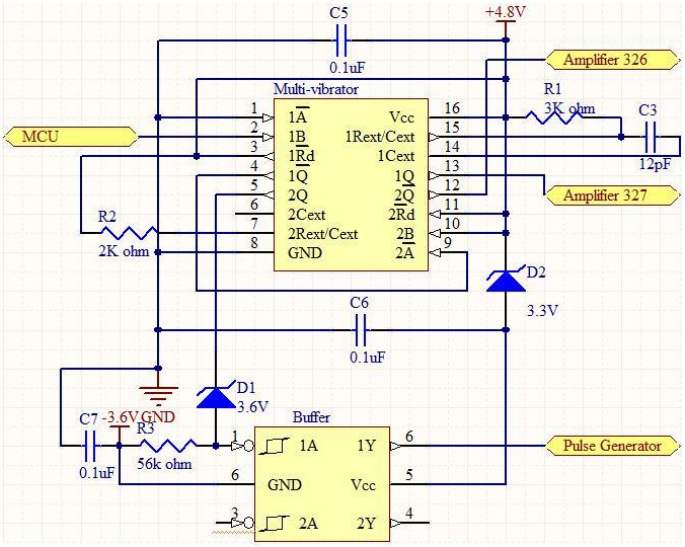

Fig. 13. The schematics of digital control unit contained in an active UWB tag

Furthermore, a buffer circuit is required to driv the UWB pulse generator. The buffer circuit is powered up from 4.8 V and -3.6 V DC. In order to simplify the circuitry, 4 batteries of 1.2 V are used to provide all the necessary DC supplies. The negative voltage is obtained by inserting a charge pump into the circuit to act as an inverter of the 3.6 V. Thus all the DC supplies in the active tag are as follows: the charge pump and the MCU are powered up by 3.6 V, and the amplifier and multi-vibrator are powered up at 4.8 V. The total current consumption is less than 5 mA from the 4.8 V batteries.

5.2 *Measured results*

A conducted emission test (into a 50 ohms load) is first conducted on the UWB tag output using an oscilloscope. The output is a Gaussian pulse train with pulse repetition frequency (PRF) of 200 kHz and peak-to-peak amplitude of 12 V, while the power consumption is only 22.8 mW. Following that, the tag is setup as a transmitter and a tapered slot antenna (TSA) (Hu et al. 2009) is used as a receiver, similar to the setup shown in Fig. 9. The time-

domain radiation performance of the active tag is investigated before and after embedding in Concrete.

The receiver antenna gain is 10 dBi. The separation between the tag and the receiver is 1 meter. The measured result with the tag before embedding in Concrete is shown in Fig. 14. The maximum signal strength is 87 mV peak to peak. Considering that the measured maximum signal input to the tag slot antenna is 12 V peak to peak, the total loss including the transmitting antenna is around 52.8 dB, which is 8.3 dB more loss than the theoretical loss value of around 44.5 dB in free space of 1 meter propagation distance. Hence the transmitter antenna gain is -8.3 dB. The reason for the low antenna gain is because it is designed to be buried in Concrete. Without the Concrete surrounding it, the resonant frequency will be incorrect and the return loss will degrade lowering the antenna gain.

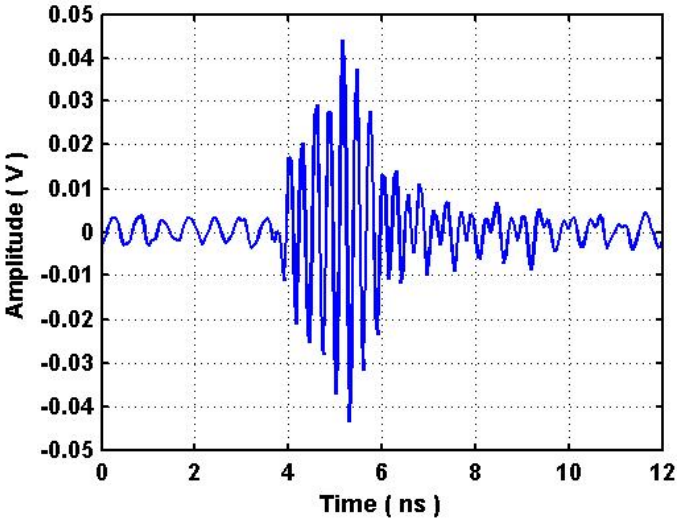

Figure 14. Measured waveform received by the tapered slot antenna when the transmitter is an active tag which is not buried in Concrete.

The received signal of the tag embedded in Concrete block of 7 × 7 × 7 cm is shown in Fig. 15 using the same measurement setup and distance separating the tag and the receiver. Fig. 15(a) shows the received pulse characteristics with the tag oriented for maximum peak-to-peak amplitude of around 116 mV. Fig. 15(b) shows the received pulse characteristics with the tag oriented for minimum peak-to-peak amplitude of around 56 mV. This decrease in amplitude of 48.3% (-6.32 dB) due to tag orientation matches with the measurement results of the proposed antenna in Section 4.2. In addition, the measurement results show that in the maximum tag antenna gain direction, the total loss at 1 meter distance is 50.3 dB. This loss is 4.8 dB more than the free space loss of 44.5 dB. This extra loss is reasonable due to the loss in Concrete.

Finally, the embedded UWB tag is employed in the debris tracking system developed by our research team, which include four UWB sensors, one locator, and tracking algorithm. Measurement results show that the maximum detection range between the active tag and four UWB sensors can be more than 190 meters.

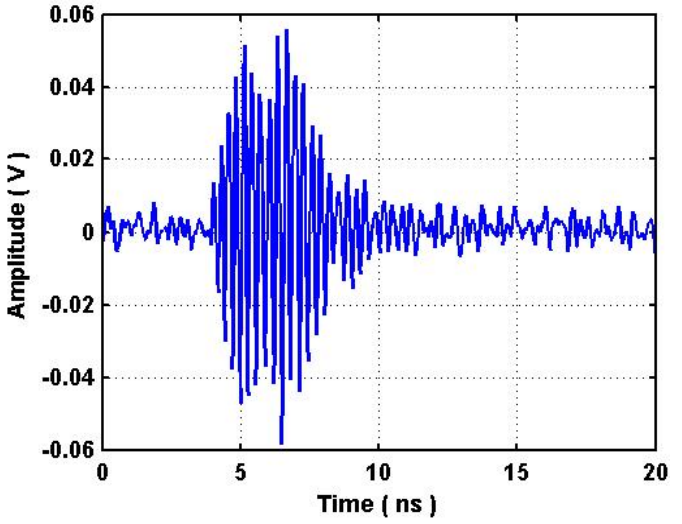

(a)

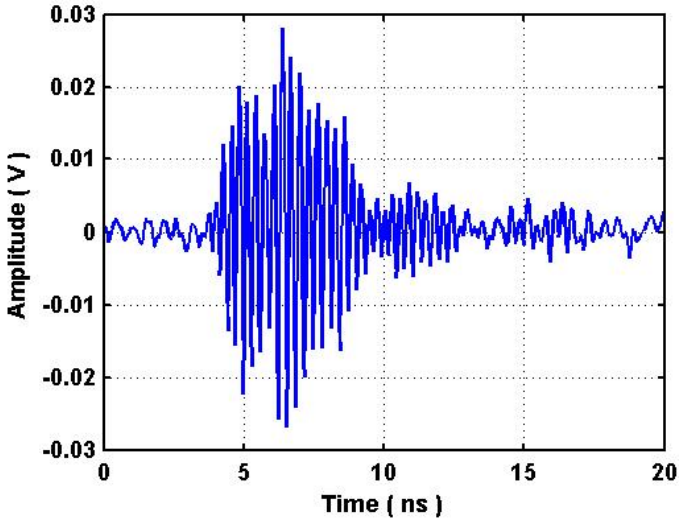

(b)

Figure 15. Measured waveform received by the tapered slot antenna when the transmitter is an active tag buried in Concrete: (a) co-polarization between the active tag and receiver, (b) cross-polarization between the active tag and receiver.

6 CONCLUSIONS AND FUTURE WORK

Due to the limitations of traditional high speed video camera, UWB technology is proposed for tracking of Concrete debris in explosion. A novel UWB slot antenna, one of the most important components in UWB tags, is designed with two measurement results of dielectric constant and loss tangent of three Concrete samples. This slot antenna embedded in Concrete is fabricated and measured with a 10-dB

return loss impedance bandwidth from 2.7 to 4.5 GHz. Time domain measurements demonstrate that the antenna can receive pulse signals both in *x-y* plane with maximum -5.83 dB variation and in *x-z* plane with that of -6.51 dB variation, respectively. A UWB tag with size of 25 × 25 × 25 mm including the integrated slot antenna is designed. The tag has very low power consumption with high output power. The tag is employed in our developed debris tracking system, covering a range of greater than 190 meters. The study in this paper shows that it is viable to implement a UWB tag including the battery to be small enough for embedding in Concrete for debris tracking.

Future work and optimization to enhance the tag include: (i) improvement to the pulse shape of the waveform received by the receiver to reduce the error in range detection; (ii) to protect the active tag against physical damage due to high stress in explosion; (iii) wireless charging / energy transfer will be investigated and employed; (iv) multiple access function to be added to enable simultaneous tracking of multiple tags.

7 ACKNOWLEDGEMENT

The authors acknowledge the helpful discussions with Prof S. C Fan of school of Civil and Environmental Engineering, NTU. This project is funded by DSTA and ASTAR SERC under Grant 052-121-0086.

REFERENCES

[1] B. Foger, C. Anders, F. Rickard, A.G. Geir, and L. Helge, “Break up Tests with Small Ammunition Houses,” Technical report, December 2006.

[2] S. Gezici, Z. Tian, G.B. Giannakis, H. Kobayashi, A.F. Molisch, H.V. Poor, and Z. Sahinoglu, “Localization via Ultra-Wideband Radios: A Look at Positioning Aspects of Future Sensor Networks,” IEEE Signal Processing Magazine, Vol. 22, No. 4, July 2005, pp 70-84.

[3] Federal Communications Commission, “FCC Report and Order for Part 15 Acceptance of Ultra Wideband (UWB) Systems from 3.1-10.6 GHz,” Washington, DC, February 2002.

[4] F.J. Aurand, “Measurements of Transient Electromagnetic Propagation through Concrete and Sand,” Sandia National Labs, Livermore, CA, September 1996.

[5] A. Muqaibel, A. Safaai-Jazi, A. Bayram, A.M. Attiya, and S.M. Riad, “Ultrawideband Through-The-Wall Propagation,” IEE Proceedings Microwave, Antennas and Propagation, December 2005, pp 581-588.

[6] Y.Z. Shen, C.L. Law, and W.B. Dou, “Ultra-Wideband Measurement of the Dielectric Constant and Loss Tangent of Concrete Slabs,” China-Japan Joint Microwave Conference, September 2008, pp 537-540.

[7] J.Y. Szw, and C.C. Chang, “Circularly Polarized Square Slot Antenna with A Pair of Inverted-L Grounded Strips,” IEEE Antennas and Wireless Propagation Letter, Vol. 7, 2008, pp 149-151.

[8] S. Hu, W.B. Dou, and C.L. Law, “A Tapered Slot Antenna with Flat and High Gain for Ultra-wideband Applications,” Journal of Electromagnetic Waves and Applications, Vol. 23, November 2009, pp 723-728.